UDC 539.4

Dynamic Stress Intensity Factor for Interfacial Cracks of Mode III Emanating from Circular Cavities in Piezoelectric Bimaterials

D. Li,[1] H. C. Wang, and L. X. Wu

Department of Civil Engineering, Hebei Jiaotong Vocational & Technical College, Shijiazhuang, China

[1] lidong242@163.com

This paper investigates dynamic stress intensity factors in piezoelectric bimaterials with interfacial cracks emanating from the circular cavities under steady SH-waves. The interfacial cracks are assumed to be permeable. Green functions for the experiment were constructed through complex variable and wave function expansion methods. Based on the crack-division and conjunction techniques, a series of Fredholm integral equations of the first kind were established to calculate the stress intensity of the crack tips. Direct numerical integration was used to solve the equations. Some numerical results were plotted to indicate the influence of the defect geometry, material constants, and SH-wave frequencies on dynamic stress intensity factors.

Keywords: dynamic stress intensity factor (DSIF), interfacial cracks, circular cavity, piezoelectric bimaterials, Green function, SH-wave.

Introduction. Piezoelectric material is popular in devices such as sensors and actuators due to its electro-mechanical coupling response. However, piezoelectric material is stiff and brittle, newly developed piezoelectric devices often fracture or fail during manufacturing or use. Therefore, researchers have explored failure behaviors caused by defects in piezoelectric material.

Narita and Shindo [1] studied the scattering problem of a harmonic SH wave from a line crack in piezoelectric material. Wang and Meguid [2] analyzed the problem of the dynamic characteristic of piezoelectricity with cracks under the anti-plane shear wave. Liu and Chen [3] investigated radial cracks originating at an elliptic cavity by the Green function method. Based on complex variable and conformal mapping methods, Wang and Gao [4] presented a novel efficient procedure for analyzing a mode III fracture problem of radial cracks emanating from a circular cavity in the piezoelectricity. Guo et al. [5, 6] analyzed the problem of two collinear cracks originating from an elliptic cavity in a piezoelectric medium. Hassan and Song [7] studied the dynamic stress intensity factors in the piezoelectric bimaterial model with two symmetrically permeable interfacial cracks near the edges of a circular hole by Green function and conjunction.

This paper investigates dynamic stress intensity factors of interfacial cracks that emanate from circular cavities in transversely isotropic piezoelectric bimaterials under steady SH-waves. It studies dynamic stress intensity factors at the crack tips through the Green function method, the crack-division, and the conjunction.

Problem Statement and Mathematical Model. Consider two well-bonded infinite transversely isotropic piezoelectric bimaterials containing $2N$ interfacial cracks emanating from N circular cavities subjected to a steady state SH-wave of frequency ω in the direction of α_0, as shown in Fig. 1. The radial crack lengths on the edge of the circular cavity j are assumed to be A_{2j-1} and A_{2j}. Values of R_j and d_j represent the radius of the circular cavity j and the distance between the crack tips, respectively. A global rectangular coordinate system xoy and N local systems $x_j o_j y_j$ are used to express the different radial cracks. The local centre of circular cavity j is c_j ($j = 1, 2, \ldots, N$). The poling direction is the positive z-axis.

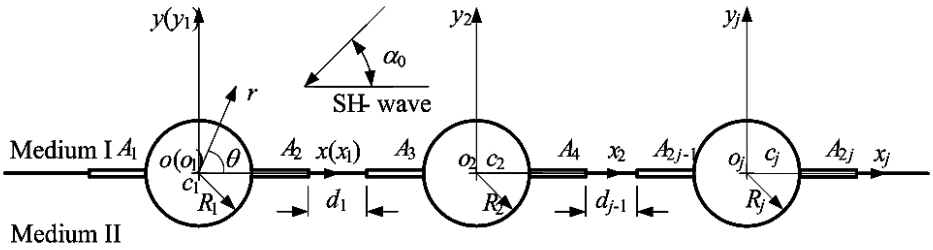

Fig. 1. Piezoelectric bimaterials with radial interface cracks emanating from the edges of circular cavities.

Many studies have explored the cracks' traction-free and permeable qualities [8, 9]; these findings were applied to the current study. The boundary conditions at the interfacial cracks' surfaces can be expressed as

$$\begin{cases} D_\theta^I(r_j,\theta_j) = D_\theta^{II}(r_j,\theta_j), \\ \tau_{\theta z}^I(r_j,\theta_j) = 0, \\ \tau_{\theta z}^{II}(r_j,\theta_j) = 0, \\ \phi^I(r_j,\theta_j) = \phi^{II}(r_j,\theta_j), \end{cases} \qquad \begin{cases} r_j \in [R_j, R_j + A_{2j-1}], & \theta_j = \pi, \\ r_j \in [R_j, R_j + A_{2j}], & \theta_j = 0. \end{cases} \tag{1}$$

The boundary continuity conditions across the interfaces of the circular cavity j can be expressed as [10]:

$$\begin{cases} \tau_{rz}^I(r_j,\theta_j) = 0, & \tau_{rz}^{II}(r_j,\theta_j) = 0, \\ \phi^I(r_j,\theta_j) = \phi^{cj}, & \phi^{II}(r_j,\theta_j) = \phi^{cj}, \\ D_r^I(r_j,\theta_j) = D_r^{cj}, & D_r^{II}(r_j,\theta_j) = D_r^{cj}, \end{cases} \qquad |\vec{r}_j| = R_j, \tag{2}$$

where D_r, D_θ, τ_{rz}, and $\tau_{\theta z}$ are two electric displacements and two shear stress components, and ϕ is the electric potential, respectively. The superscript cj indicates the quantities in the circular cavity j, and the superscripts I and II indicate quantities in upper and under half-spaces, respectively.

The steady-state electromechanical field quantities will generally involve a time factor $\exp(-i\omega t)$ as follows:

$$P^*(x, y, t) = P(x, y)e^{-i\omega t}, \tag{3}$$

where P^* and P express the desired field variable and the amplitude of field quantities, respectively. The time factor $\exp(-i\omega t)$ will henceforth be omitted in all the following expressions.

Under the dynamic anti-plane loading, the governing equations of linear piezoelectricity can be expressed as [2]:

$$c_{44}\nabla^2 w + e_{15}\nabla^2\phi + \rho\omega^2 w = 0, \qquad e_{15}\nabla^2 w - \kappa_{11}\nabla^2\phi = 0, \tag{4}$$

where c_{44}, e_{15}, and κ_{11} are the elastic modulus, the piezoelectric constant, and the dielectric constant, while ρ and w are the mass density of the material and the anti-plane displacement, respectively.

A new function is defined

$$\varphi = \phi - \frac{e_{15}}{\kappa_{11}} w. \tag{5}$$

Equation (4) can be further simplified into

$$\nabla^2 w + k^2 w = 0, \qquad \nabla^2 \varphi = 0, \tag{6}$$

in which k is the wave number and the expression is

$$k^2 = \frac{\rho \omega^2}{c^*}, \tag{7}$$

where c^* is the effective modulus of the material defined as

$$c^* = c_{44}(1+\lambda), \tag{8}$$

with

$$\lambda = \frac{e_{15}^2}{c_{44}\kappa_{11}} \tag{9}$$

being a normalized piezoelectric constant.

Introducing a complex variable $\eta = x + iy = re^{i\theta}$ and its conjugate $\overline{\eta} = x - iy = re^{-i\theta}$, Eq. (6) can be rewritten as [11]:

$$\frac{\partial^2 w}{\partial \eta \partial \overline{\eta}} + \frac{1}{4} k^2 w = 0, \qquad \frac{\partial^2 \varphi}{\partial \eta \partial \overline{\eta}} = 0. \tag{10}$$

The constitutive laws for the piezoelectricity in complex plane (η, $\overline{\eta}$) can be written as

$$\begin{aligned}
\tau_{rz} &= c_{44}\left(\frac{\partial w}{\partial \eta} e^{i\theta} + \frac{\partial w}{\partial \overline{\eta}} e^{-i\theta}\right) + e_{15}\left(\frac{\partial \phi}{\partial \eta} e^{i\theta} + \frac{\partial \phi}{\partial \overline{\eta}} e^{-i\theta}\right), \\
\tau_{\theta z} &= ic_{44}\left(\frac{\partial w}{\partial \eta} e^{i\theta} - \frac{\partial w}{\partial \overline{\eta}} e^{-i\theta}\right) + ie_{15}\left(\frac{\partial \phi}{\partial \eta} e^{i\theta} - \frac{\partial \phi}{\partial \overline{\eta}} e^{-i\theta}\right), \\
D_r &= e_{15}\left(\frac{\partial w}{\partial \eta} e^{i\theta} + \frac{\partial w}{\partial \overline{\eta}} e^{-i\theta}\right) - \kappa_{11}\left(\frac{\partial \phi}{\partial \eta} e^{i\theta} + \frac{\partial \phi}{\partial \overline{\eta}} e^{-i\theta}\right), \\
D_\theta &= ie_{15}\left(\frac{\partial w}{\partial \eta} e^{i\theta} - \frac{\partial w}{\partial \overline{\eta}} e^{-i\theta}\right) - i\kappa_{11}\left(\frac{\partial \phi}{\partial \eta} e^{i\theta} - \frac{\partial \phi}{\partial \overline{\eta}} e^{-i\theta}\right).
\end{aligned} \tag{11}$$

Green Function Solution. Set up a couple of electro-mechanical Green functions G_w and G_ϕ, which are basic solutions of displacement and electric potential for a semi-infinite piezoelectric material with N semi-circular notches subject to a time harmonic anti-plane line force $\delta(\eta - \eta_0)$ at an arbitrary position η_0 on the interface. The total solution can be decomposed into the incident and the scattering fields, respectively, which can be written as [3]:

$$G_w^{(i)} = \frac{i}{2c_{44}(1+\lambda)} H_0^{(1)}(k|\eta - \eta_0|), \qquad G_\phi^{(i)} = \frac{e_{15}}{\kappa_{11}} G_w^{(i)}, \tag{12}$$

and

$$\begin{aligned} G_w^{(s)} &= \sum_{j=1}^{N} \sum_{m=-\infty}^{\infty} A_m^j H_m^{(1)}(k|\eta_j|) \left[\left(\frac{\eta_j}{|\eta_j|} \right)^m + \left(\frac{\eta_j}{|\eta_j|} \right)^{-m} \right], \\ G_\phi^{(s)} &= \frac{e_{15}}{\kappa_{11}} G_w^{(s)} + \sum_{j=1}^{N} \sum_{m=1}^{\infty} [B_m^j \eta_j^{-m} + C_m^j \bar{\eta}_j^{-m}], \end{aligned} \tag{13}$$

where the superscripts i and s represent the incident and the scattering quantities, while $H_m^{(1)}$ expresses the Hankel function of the first kind, respectively.

Therefore, the coupled Green functions G_w and G_ϕ can be given by

$$G_w = G_w^{(i)} + G_w^{(s)}, \qquad G_\phi = G_\phi^{(i)} + G_\phi^{(s)}. \tag{14}$$

In the semi-circular notch j, there is only the electric potential, which can be expressed as

$$G_\phi^{cj} = D_0 + \sum_{m=1}^{\infty} [D_m^j \eta_j^m + E_m^j \bar{\eta}_j^m]. \tag{15}$$

The unknown constants A_m^j, B_m^j, C_m^j, D_m^j, and E_m^j can be achieved by the boundary conditions (2).

Equation (14) gives the coupled Green functions in the two semi-infinite materials.

Dynamic Electro-Elastic Fields. The piezoelectric bimaterials are subjected to a steady state SH-wave with an incident angle α_0 in the upper half-space. The anti-plane elastic displacement $w^{(i)}$ and the inplane electric potential $\phi^{(i)}$ of the incident wave can be described as

$$\begin{aligned} w^{(i)} &= w_0 \exp\left[-i \frac{k_I}{2} (\eta e^{-i\alpha_0} + \bar{\eta} e^{i\alpha_0}) \right], \\ \phi^{(i)} &= \phi_0 \exp\left[-i \frac{k_I}{2} (\eta e^{-i\alpha_0} + \bar{\eta} e^{i\alpha_0}) \right]. \end{aligned} \tag{16}$$

Because of the interface, a reflected wave and a transmitted wave will be caused in the upper half-space medium I and the under half-space medium II. The expressions of the reflected fields and the transmitted fields can be written respectively as [12]:

$$\begin{aligned} w^{(r)} &= w_1 \exp\left[-i \frac{k_I}{2} (\eta e^{i\alpha_0} + \bar{\eta} e^{-i\alpha_0}) \right], \\ \phi^{(r)} &= \phi_1 \exp\left[-i \frac{k_I}{2} (\eta e^{i\alpha_0} + \bar{\eta} e^{-i\alpha_0}) \right], \end{aligned} \tag{17}$$

$$w^{(t)} = w_2 \exp\left[-i \frac{k_{II}}{2} (\eta e^{-i\alpha_2} + \bar{\eta} e^{i\alpha_2}) \right], \tag{18a}$$

$$\phi^{(t)} = \phi_2 \exp\left[-i\frac{k_{II}}{2}(\eta e^{-i\alpha_2} + \overline{\eta} e^{i\alpha_2})\right]. \tag{18b}$$

Scattering fields occur due to the circular cavities in the piezoelectric material. The scattering fields are caused by the incident, the reflected and the transmitted fields can be written respectively as

$$\begin{aligned} w^{(is)} &= \sum_{j=1}^{N}\sum_{m=-\infty}^{\infty} {}^{j}A_m^{(is)} H_m^{(1)}(k_I|\eta_j|)\left(\frac{\eta_j}{|\eta_j|}\right)^m, \\ \phi^{(is)} &= \frac{e_{15}^I}{\kappa_{11}^I} w^{(is)} + \sum_{j=1}^{N}\sum_{m=1}^{+\infty} {}^{j}B_m^{(is)} \eta_j^{-m} + \sum_{j=1}^{N}\sum_{m=1}^{+\infty} {}^{j}C_m^{(is)} \overline{\eta}_j^{-m}, \end{aligned} \tag{19}$$

$$\begin{aligned} w^{(rs)} &= \sum_{j=1}^{N}\sum_{m=-\infty}^{\infty} {}^{j}A_m^{(rs)} H_m^{(1)}(k_I|\eta_j|)\left(\frac{\eta_j}{|\eta_j|}\right)^m, \\ \phi^{(rs)} &= \frac{e_{15}^I}{\kappa_{11}^I} w^{(rs)} + \sum_{j=1}^{N}\sum_{m=1}^{+\infty} {}^{j}B_m^{(rs)} \eta_j^{-m} + \sum_{j=1}^{N}\sum_{m=1}^{+\infty} {}^{j}C_m^{(rs)} \overline{\eta}_j^{-m}, \end{aligned} \tag{20}$$

$$\begin{aligned} w^{(ts)} &= \sum_{j=1}^{N}\sum_{m=-\infty}^{\infty} {}^{j}A_m^{(ts)} H_m^{(1)}(k_{II}|\eta_j|)\left(\frac{\eta_j}{|\eta_j|}\right)^m, \\ \phi^{(ts)} &= \frac{e_{15}^{II}}{\kappa_{11}^{II}} w^{(ts)} + \sum_{j=1}^{N}\sum_{m=1}^{+\infty} {}^{j}B_m^{(ts)} \eta_j^{-m} + \sum_{j=1}^{N}\sum_{m=1}^{+\infty} {}^{j}C_m^{(ts)} \overline{\eta}_j^{-m}. \end{aligned} \tag{21}$$

The summation of the total electric-elastic fields in the upper half-space medium I and the under half-space medium II are

$$w^I = w^{(i)} + w^{(is)} + w^{(r)} + w^{(rs)}, \qquad \phi^I = \phi^{(i)} + \phi^{(is)} + \phi^{(r)} + \phi^{(rs)}, \tag{22}$$

and

$$w^{II} = w^{(t)} + w^{(ts)}, \qquad \phi^{II} = \phi^{(t)} + \phi^{(ts)}. \tag{23}$$

Only the electric fields exist in the circular cavities. The expressions of the circular cavity j, which are caused by the incident, the reflected and the transmitted fields can be written as follows, respectively:

$$\phi_j^{ic} = {}^{j}D_0^{(is)} + \sum_{m=1}^{\infty}[{}^{j}D_m^{(is)}\eta_j^m + {}^{j}E_m^{(is)}\overline{\eta}_j^m], \tag{24}$$

$$\phi_j^{rc} = {}^{j}D_0^{(rs)} + \sum_{m=1}^{\infty}[{}^{j}D_m^{(rs)}\eta_j^m + {}^{j}E_m^{(rs)}\overline{\eta}_j^m], \tag{25}$$

$$\phi_j^{tc} = {}^{j}D_0^{(ts)} + \sum_{m=1}^{\infty}[{}^{j}D_m^{(ts)}\eta_j^m + {}^{j}E_m^{(ts)}\overline{\eta}_j^m]. \tag{26}$$

The unknown constants can be solved by the conditions at the edge of the circular cavity j.

Integral Equations and DSIFs. The integral equation can be established by using the conjunction method combined with the crack-division technique according to the obtained Green functions and the total electric-elastic fields. Figure 2 shows the conjunction for the piezoelectric bimaterials with $2N$ semi-circular notches.

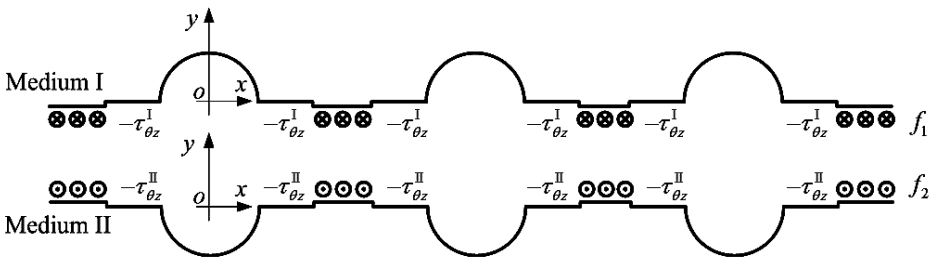

Fig. 2. Conjunction for piezoelectric bimaterials with $2N$ semi-circular notches.

Firstly, consider that the piezoelectric materials have $2N$ circular cavities at the interface without radial cracks. The finite piezoelectric media is taken into two half-space media. To overcome this and achieve traction-free and electric permeable cracks, two negative shear stresses $[-\tau^{I}_{\theta z}]$ and $[-\tau^{II}_{\theta z}]$ are applied on the crack locations.

Secondly, the additional shear stresses disturb the continuity conditions on the interface. A dual of additional unknown shear stresses f_1 and f_2 are applied on the surfaces of the upper and the under half-space, respectively, to meet the perfectly bonded interface. Thus, the continuity conditions of shear stresses and displacements on the perfectly bonded interface without the locations of the circular cavities and the interfacial cracks can be expressed as

$$\tau^{I}_{\theta z}\cos\theta_0 + f_1 = \tau^{II}_{\theta z}\cos\theta_0 + f_2, \tag{27}$$

and

$$w^{I} + w^{(f_1)} + w^{(cI)} = w^{II} + w^{(f_2)} + w^{(cII)}, \tag{28}$$

where

$$w^{(f_1)} = \int_{R_1+A_1}^{\infty} f_1(r_{01}, \pi) G^{I}_{w}(r_1, \theta_1; r_{01}, \pi)\, dr_{01} +$$

$$+ \sum_{j=1}^{N-1} \int_{R_j+A_{2j}}^{R_j+A_{2j}+d_j} f_1(r_{0j}, 0) G^{I}_{w}(r_j, \theta_j; r_{0j}, 0)\, dr_{0j} +$$

$$+ \int_{R_N+A_{2N}}^{\infty} f_1(r_{0N}, 0) G^{I}_{w}(r_N, \theta_N; r_{0N}, 0)\, dr_{0N}, \tag{29}$$

$$w^{(f_2)} = -\int_{R_1+A_1}^{\infty} f_2(r_{01}, \pi) G^{II}_{w}(r_1, \theta_1; r_{01}, \pi)\, dr_{01} -$$

$$- \sum_{j=1}^{N-1} \int_{R_j+A_{2j}}^{R_j+A_{2j}+d_j} f_2(r_{0j}, 0) G^{II}_{w}(r_j, \theta_j; r_{0j}, 0) dr_{0j} -$$

$$- \int_{R_N+A_{2N}}^{\infty} f_2(r_{0N}, 0) G^{II}_{w}(r_N, \theta_N; r_{0N}, 0)\, dr_{0N}, \tag{30}$$

$$w^{(cI)} = \sum_{j=1}^{N} \int_{R_j}^{R_j + A_{2j-1}} \tau_{\theta z}^{(I)}(r_{0j}, \pi) G_w^I(r_j, \theta_j; r_{0j}, \pi) dr_{0j} -$$

$$- \sum_{j=1}^{N} \int_{R_j}^{R_j + A_{2j}} \tau_{\theta z}^{(I)}(r_{0j}, 0) G_w^I(r_j, \theta_j; r_{0j}, 0) dr_{0j}, \tag{31}$$

$$w^{(cII)} = - \sum_{j=1}^{N} \int_{R_j}^{R_j + A_{2j-1}} \tau_{\theta z}^{(II)}(r_{0j}, \pi) G_w^{II}(r_j, \theta_j; r_{0j}, \pi) dr_{0j} +$$

$$+ \sum_{j=1}^{N} \int_{R_j}^{R_j + A_{2j}} \tau_{\theta z}^{(II)}(r_{0j}, 0) G_w^{II}(r_j, \theta_j; r_{0j}, 0) dr_{0j}. \tag{32}$$

Substituting equations (22), (23), and (27) into (28), the integral equations to calculate the unknown stress $f_1(r_0, \theta_0)$ can be obtained as follows:

$$\int_{R_1 + A_1}^{\infty} f_1(r_{01}, \pi)[G_w^I(r_1, \theta_1; r_{01}, \pi) + G_w^{II}(r_1, \theta_1; r_{01}, \pi)] dr_{01} +$$

$$+ \sum_{j=1}^{N-1} \int_{R_j + A_{2j}}^{R_j + A_{2j} + d_j} f_1(r_{0j}, 0)[G_w^I(r_j, \theta_j; r_{0j}, 0) + G_w^{II}(r_j, \theta_j; r_{0j}, 0)] dr_{0j} +$$

$$+ \int_{R_N + A_{2N}}^{\infty} f_1(r_{0N}, 0)[G_w^I(r_N, \theta_N; r_{0N}, 0) + G_w^{II}(r_N, \theta_N; r_{0N}, 0)] dr_{0N} =$$

$$= w^{(ts)}(r_j, \theta_j) - w^{(is)}(r_j, \theta_j) - w^{(rs)}(r_j, \theta_j) +$$

$$+ \int_{R_1 + A_1}^{\infty} [\tau_{\theta z}^I(r_{01}, \pi) - \tau_{\theta z}^{II}(r_{01}, \pi)] G_w^{II}(r_1, \theta_1; r_{01}, \pi) dr_{01} -$$

$$- \sum_{j=1}^{N-1} \int_{R_j + A_{2j}}^{R_j + A_{2j} + d_j} [\tau_{\theta z}^I(r_{0j}, 0) - \tau_{\theta z}^{II}(r_{0j}, 0)] G_w^{II}(r_j, \theta_j; r_{0j}, 0) dr_{0j} -$$

$$- \int_{R_N + A_{2N}}^{\infty} [\tau_{\theta z}^I(r_{0N}, 0) - \tau_{\theta z}^{II}(r_{0N}, 0)] G_w^{II}(r_N, \theta_N; r_{0N}, 0) dr_{0N} -$$

$$- \sum_{j=1}^{N} \int_{R_j}^{R_j + A_{2j-1}} \tau_{\theta z}^I(r_{0j}, \pi) G_w^I(r_j, \theta_j; r_{0j}, \pi) dr_{0j} +$$

$$+ \sum_{j=1}^{N} \int_{R_j}^{R_j + A_{2j}} \tau_{\theta z}^I(r_{0j}, 0) G_w^I(r_j, \theta_j; r_{0j}, 0) dr_{0j} -$$

$$- \sum_{j=1}^{N} \int_{R_j}^{R_j + A_{2j-1}} \tau_{\theta z}^{II}(r_{0j}, \pi) G_w^{II}(r_j, \theta_j; r_{0j}, \pi) dr_{0j} +$$

$$+\sum_{j=1}^{N}\int_{R_j}^{R_j+A_{2j}} \tau_{\theta z}^{II}(r_{0j},\,0)G_w^{II}(r_j,\,\theta_j;\,r_{0j},\,0)dr_{0j}. \tag{33}$$

Defining a normalized dynamic stress intensity factor k_3^{σ} at the left and the right interfacial crack tips of the circular cavity j, the expression is given by

$$k_3^{\sigma} = \frac{1}{\tau_0 Q}\left|\lim_{r_0 \to R_j + A} f_1(r_{0j},\,\theta_{0j})\sqrt{2(r_0 - R_j - A)}\right|, \quad A = A_{2j-1}, A_{2j}\,(j = 1,\,2,\,\ldots,\,N), \tag{34}$$

where Q is the characteristic parameter, and τ_0 is the shear stress magnitude of the transmitted wave. They can respectively be expressed as follows [13]:

$$Q = \sqrt{(A+R_j)^4 - R_j^4}\Big/\sqrt{(A+R_j)^3}, \tag{35}$$

$$\tau_0 = -ik_{II}(c_{44}^{II}w_2 + e_{15}^{II}\phi_2). \tag{36}$$

Results and Discussion. In the following examples, it is assumed that there are two circular cavities with equal radii, and the crack lengths emanating from the edges of the circular cavities are also equal to each other, as shown in Fig. 3. Some numerical examples at the left and the right crack tips are plotted on the left circular cavity to show the influence of defect geometry, material constants, and SH-wave frequencies on dynamic stress intensity factors.

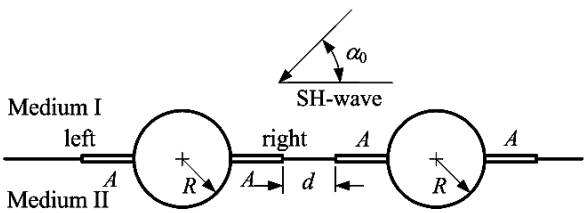

Fig. 3. Piezoelectric bimaterials with interfacial radial cracks emanating from the edges of two circular cavities.

Figure 4 shows the variations of the DSIFs at the left and the right tips of the radial cracks with different crack lengths A. First, we restrict our attention to the case $A/R = 1000$ when the radius R is very small. The curve at the right tip of the radial crack gives compared with the results of the document [12], indicating that they coincide. The right tip gives larger DSIFs values than the left tip. For both tips, the DSIFs have larger values at lower frequencies rather than higher frequencies. As crack length increases, the DSIFs at the right tip decrease and the left tip appears the oscillation phenomenon.

Figure 5 shows DSIFs oscillations with different piezoelectric constants λ_I. At the right tip, the increase in the piezoelectric constants λ_I leads to the decrease in the DSIFs, and the peak values appear when $k_I R$ is almost at 0.3–0.5. With the increase of piezoelectric constants, the value of DSIFs at the left tips increase at the range $k_I R = 0$–0.7, but there is a reverse trend when $k_I R > 0.7$.

Figure 6 shows the variation of the DSIFs with different crack lengths A and piezoelectric constants λ_I. It can be seen that the DSIFs is largest when the crack length A has the similar size with the cavity's radius R. The values of DSIFs increase with the

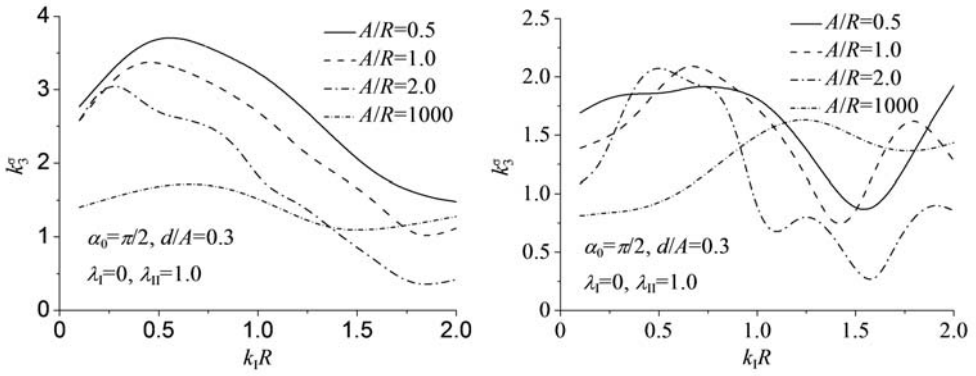

Fig. 4. Influence of $k_I R$ on DSIFs of the interfacial cracks' tips under different A/R: (a) right tip; (b) left tip.

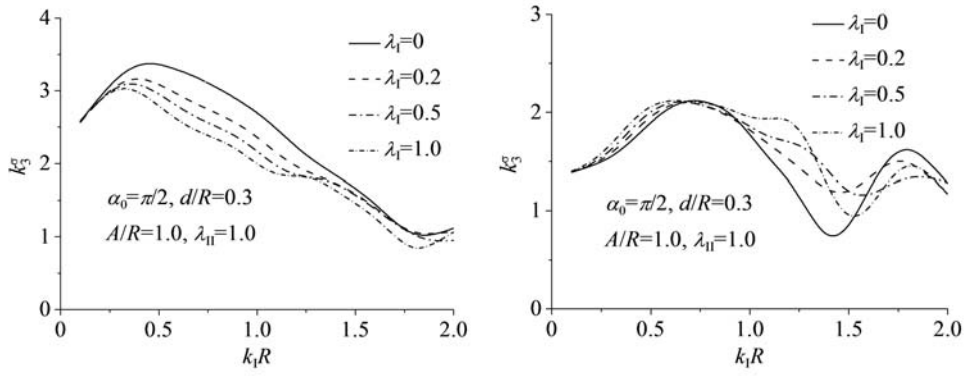

Fig. 5. Influence of $k_I R$ on DSIFs of the interfacial cracks' tips under different λ_I: (a) right tip; (b) left tip.

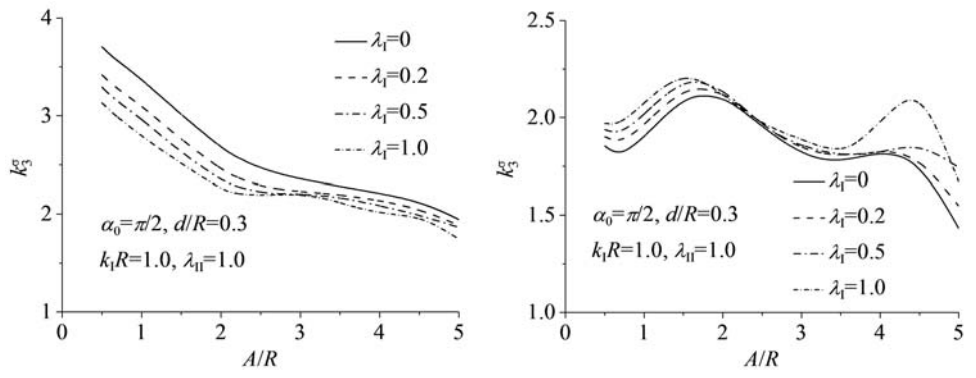

Fig. 6. Influence of A/R on DSIFs of the interfacial cracks' tips under different λ_I: (a) right tip; (b) left tip.

decrease of A/R at the right tip. DSIFs peaks at the left tip are observed when $A/R = 1.5$–1.8.

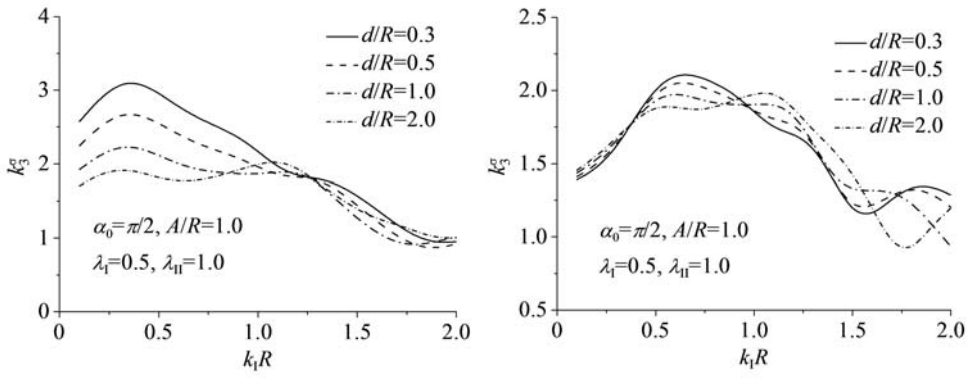

Fig. 7. Influence of $k_I R$ on DSIFs of the interfacial cracks' tips under different d/R: (a) right tip; (b) left tip.

Figure 7 shows the effect of the distances between the two radial cracks. The DSIFs values increase with the decrease of the distance d when $k_I R < 1.0$ at the right tip. At the left tip, with the increase of the distance d the DSIFs increase when $k_I R < 0.4$; however, when $k_I R = 0.4$–1.0, there is a reverse trend. Oscillation appears when $k_I R > 1.0$ at both tips.

Conclusions. This paper gives a theoretical solution to dynamic stress intensity factors for interfacial radial cracks emanating from the edges of the circular cavities in piezoelectric bimaterials under the steady state SH-waves. The formulation is established through the Green function method, crack-division and conjunction techniques. The results indicate that the increase in the distance between the crack's tips decreases the DSIFs. The right tip gives larger dynamic stresses intensity than the left tip. The influence of the cavity on DSIFs is more significant when the crack lengths have similar sizes to the circular cavities' radii. Dynamic analyses in piezoelectric bimaterials are more important than homogenous piezoelectricity, because the former may have larger dynamic stress intensity factors. The DSIFs have larger values at lower frequencies rather than higher frequencies, so we must pay more attention to the fractures at low frequencies. This paper can suggest a useful reference for investigating piezoelectric bimaterials with more complicated interfacial faults as well as in the design of piezoelectric structures.

Acknowledgments. The authors are grateful for the support of the National Science Fund for Young Scholars of Hebei Education Department (Q2012031).

1. F. Narita and Y. Shindo, "Dynamic anti-plane shear of a cracked piezoelectric ceramic," *Theor. Appl. Fract. Mech.*, **29**, 169–180 (1998).
2. X. D. Wang and S. A. Meguid, "Modelling and analysis of the dynamic behaviour of piezoelectric materials containing interacting cracks," *Mech. Mater.*, **32**, 723–737 (2000).
3. D. Liu and Z. Chen, "Scattering of SH-wave by cracks originating at an elliptic hole and dynamic stress intensity factor," *Appl. Math. Mech.*, **25**, No. 9, 1047–1056 (2004).
4. Y. J. Wang and C. F. Gao, "The mode III cracks originating from the edge of a circular hole in a piezoelectric solid," *Int. J. Solids Struct.*, **45**, 4590–4599 (2008).
5. J. H. Guo, Z. X. Lu, H. T. Han, and Z. Yang, "Exact solutions for anti-plane problem of two asymmetrical edge cracks emanating from an elliptical hole in a piezoelectric material," *Int. J. Solids Struct.*, **46**, 3799–3809 (2009).

6. J. H. Guo, Z. X. Lu, H. T. Han, and Z. Yang, "The behavior of two non-symmetrical permeable cracks emanating from an elliptical hole in a piezoelectric solid," *Eur. J. Mech. – A/Solids*, **29**, 654–663 (2010).
7. A. Hassan and T. S. Song, "Dynamic anti-plane analysis for two symmetrically interfacial cracks near circular cavity in piezoelectric bi-materials," *Appl. Math. Mech*., **35**, No. 10, 1261–1270 (2014).
8. M. Dunn, "The effect of crack face boundary conditions on the fracture mechanica of piezoelectric solids," *Eng. Fract. Mech.*, **48**, 25–39 (1994).
9. T. Y. Zhang, C. F. Qian, and P. Tong, "Linear electro-elastic analysis of a cavity or a crack in a piezoelectric material," *Int. J. Solids Struct.*, **35**, 2121–2149 (1998).
10. H. Sosa and N. Khutoryansky, "New developments concerning piezoelectric materials with defects," *Int. J. Solids Struct.*, **33**, 3399–3414 (1996).
11. D. K. Liu and H. Lin, "Scattering of SH-waves by an interacting interface linear crack and a circular cavity near bimaterial interface," *Acta Mech. Sinica*, **20**, No. 3, 317–326 (2004).
12. X. D. Wang, "On the dynamic behaviour of interacting interfacial cracks in piezoelectric media," *Int. J. Solids Struct.*, **38**, 815–831 (2001).
13. G. C. Sih, "Stress distribution near internal crack tips for longitudinal shear problems," *J. Appl. Mech.*, **32**, No. 1, 51–58 (1965).

Received 03. 08. 2015